http://www.jstage.jst.go.jp/browse/biophysics

BIOPHYSICS

Vol. 9, pp. 37–49 (2013)
doi: 10.2142/biophysics.9.37

Characterization of the ordered phase formed by sphingomyelin analogues and cholesterol binary mixtures

Masanao Kinoshita[1,2], Sarah Goretta[3], Hiroshi Tsuchikawa[3], Nobuaki Matsumori[1,3] and Michio Murata[1,2,3]

[1]*JST ERATO, Lipid Active Structure Project, Osaka University, 1-1 Machikaneyama, Toyonaka, Osaka 560-0043, Japan*
[2]*Project Research Center for Fundamental Science, Osaka University, 1-1 Machikaneyama, Toyonaka, Osaka 560-0043, Japan*
[3]*Department of Chemistry, Graduate School of Science, Osaka University, 1-1 Machikaneyama, Toyonaka, Osaka 560-0043, Japan*

Received February 21, 2013; accepted April 2, 2013

The influences of structural alterations of sphingomyelin (SM) on its interactions with cholesterol (chol) and on ordered phase formation were examined by density measurements and surface pressure vs. molecular area isotherm measurements. In addition, we quantitatively characterized the ordered phase formed in each SM and chol binary mixture on the basis of the molecular compressional modulus of SM (C_{mol}^{-1}). Density measurements demonstrated that the ordered phase formation in *threo*-SM (tSM)/chol and dihydrosphingomyelin (DHSM)/chol binary bilayers shows similar chol concentration-dependency to that of natural *erythro*-SM (eSM)/chol bilayers; the ordered phase formation was completed in the presence of 25 mol% chol. In contrast, SM bearing a triple bond in the place of a double bond (tripleSM) required a greater concentration of chol to completely transform the bilayer into the ordered phase (at 40 mol% chol). Surface pressure vs. molecular area isotherms showed that the DHSM molecule (C_{mol}^{-1}=290 mN/m) is more rigid than eSM (C_{mol}^{-1}=240 mN/m) above 30 mol% chol (in the ordered phase), although these values are similar (140–150 mN/m) in the absence of chol (liquid condensed phase). Most likely, the DHSM/chol mixture forms a more ordered membrane than the eSM/chol mixture does. Moreover, in the absence of chol, the rigidity of the tripleSM molecule (C_{mol}^{-1}=250 mN/m) is significantly higher as compared with that of the eSM molecule (C_{mol}^{-1}=150 mN/m), which is probably due to the presence of a triple bond.

Key words: density measurement, partial molecular volume, π-A isotherm, monolayer, molecular compressional modulus

Corresponding author: Masanao Kinoshita, JST ERATO, Lipid Active Structure Project, Osaka University, Machikaneyama 1-1, Toyonaka, Osaka, 560-0043, Japan and Project research Center for Fundamental Science, Osaka University, Machikaneyama 1-1, Toyonaka, Osaka, 560-0043, Japan.
e-mail: kinoshi@chem.sci.osaka-u.ac.jp;
Michio Murata, JST ERATO, Lipid Active Structure Project, Osaka University, Machikaneyama 1-1, Toyonaka, Osaka, 560-0043, Japan and Project research Center for Fundamental Science, Osaka University, Machikaneyama 1-1, Toyonaka, Osaka, 560-0043, Japan. Department of Chemistry, Graduate School of Science, Osaka University, 1-1 Machikaneyama, Toyonaka, Osaka 560-0043, Japan.
e-mail: murata@chem.sci.osaka-u.ac.jp

Sphingomyelin (SM) is a major component of the outer leaflet of cellular plasma membranes and is involved in lateral heterogeneity and raft formation together with cholesterol (chol), which is also enriched in mammalian plasma membranes[1–4].

The most abundant naturally occurring SM is D-*erythro*-(2*S*,3*R*)-sphingomyelin (eSM), which has a phosphocholine headgroup linked to the hydroxyl group on C1 of a long sphingosin chain, bearing a fatty acyl group *via* an amide group on C2 (Fig. 1a) (reviewed by Barenholz, 1984)[5]. Model membrane systems have provided fundamental information on the interactions between eSM and chol; the addition of chol to eSM bilayers in the fluid phase causes the formation of an ordered phase, called the liquid-ordered (Lo) phase[6–8], which has physical properties similar to those of the raft as reviewed previously[9]. Interactions between eSM and chol in

©2013 THE BIOPHYSICAL SOCIETY OF JAPAN

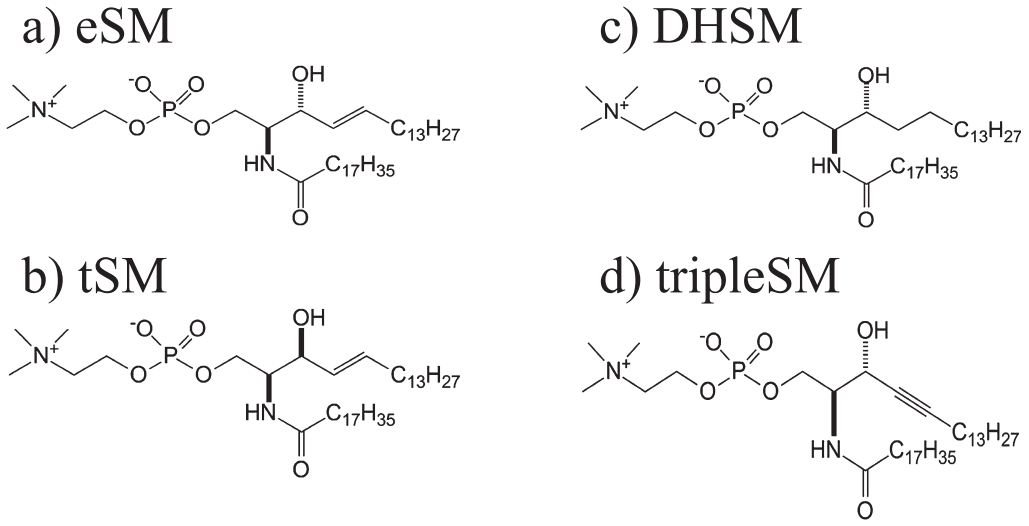

Figure 1 Schematic models of (a) *erythro*-sphingomyelin (eSM), (b) *threo*-sphingomyelin (tSM), (c) dihydrosphingomyelin (DHSM), and (d) (2*S*,3*S*)-{2-[(2-hexadecanoylamino-3-hydroxyoctadec-4-ynyloxy)-hydroxyphosphoryloxy]ethyl}trimethylammonium (tripleSM). All sphingomyelins contained a C18:0 hydrocarbon chain.

the Lo phase are attributed to several factors, such as the network of weak hydrogen bonds[10] and steric matching that allow the large polar headgroups of eSM to "cover" a chol molecule to prevent the exposure of its nonpolar portion to water[11]. The steric matching between lipid molecules is referred to as the umbrella model[2]. These intermolecular interactions between eSM and chol also may function in biological systems to segregate microdomains from the surrounding fluid matrix. Therefore, information on the membrane properties of SM and its interaction with chol is important for understanding membrane heterogeneity and lipid raft formation.

Previous studies have disclosed that conformational alterations of an SM molecule around the interfacial region often affect its membrane properties. For example, L-*threo*-(2*S*,3*S*)-sphingomyelin (tSM), which is an epimer of eSM at the hydroxy bearing C3 position, exhibits a different thermal phase behavior from that of an eSM bilayer (Fig. 1b). Bruzik and Tsai reported that the main transition temperature of a C18:0-tSM bilayer is 0.5°C lower than that of a C18:0-eSM bilayer[12]. Moreover, differential scanning calorimetry (DSC) results showed that a C18:0-tSM bilayer transforms into the subgel phase through metastable phases different from those of a C18:0-eSM bilayer. In the gel phase, the rotational motion about the C1–C2 bond is restricted in eSM while this restriction effect was not obvious for tSM[13]. Thus, the mobility of an SM molecule at the membrane interface is likely to contribute to the difference in phase behaviors between eSM and tSM. Although the membrane properties of pure tSM bilayers have already been reported, the influence of chol on the membrane features remains unknown. Considering that the synthetic SMs frequently used for a model membrane in previous studies are a mixture of eSM and tSM, information on the intermolecular interaction between tSM and chol is equally important as that between eSM and chol[14].

Dihydrosphingomyelin (DHSM) is a minor sphingomyelin (5–10% of all sphingomyelins) in cultured cells, *i.e.*, human skin fibroblasts and baby hamster kidney cells (Fig. 1c)[14]. In contrast, DHSM accounts for 50% of all phospholipids in the human lens membrane[15]. Considering that chol is also enriched in the human lens, DHSM is expected to have specific interactions with chol. Kuikka *et al*. reported that C16:0-DHSM bilayers in the presence of chol form more ordered domains than comparable C16:0-SM/chol bilayers, as evidenced by their DPH quenching measurements[16]. Fluorescence microscopic observations also suggested that, in giant unilamellar vesicles (GUV) consisting of C16:0-DHSM/egg-PC/egg-PE/chol at a 1:1:1:1 molar ratio, C16:0-DHSM in the presence of chol forms a solid phase at room temperature, which is more ordered than the Lo phase[17]. On the other hand, the replacement of C16:0-DHSM by the egg-SM (mainly consisting of C16:0-eSM) leads to the Lo phase formation instead of the solid phase. Thus, the authors suggested that DHSM contacts more favorably with chol than eSM does. In addition, there are some reports on lipid packing in pure DHSM membranes; Kuikka *et al*. revealed that pure C16:0-DHSM exhibits packing behavior similar to C16:0-SM using surface pressure vs. molecular area isotherm (π-*A* isotherm) measurements[16]. On the other hand, Nyholm *et al*. demonstrated that membrane resistance to partitioning of a fluorescent dye, prodan, is in the order C16:0-DHSM>DPPC>C16:0-eSM, and suggested that DHSM forms more ordered bilayers of the liquid crystalline (fluid) phase than eSM does[18]. Speculatively, DHSM-induced strong hydrogen bond contributes to the ordering of the hydrocarbon chains both in the presence and/or absence of chol[18].

On the other hand, it is speculated that the difference in the structural influence on SM-chol interaction is not so clear between eSM, tSM and DHSM, if any, because their hydrocarbon chains basically take similar zigzag conformation, albeit their mobility being much different. In order to obtain clear evidence that the interfacial structures of SM affects the SM-chol interaction, we synthesized (2*S*,3*S*)-{2-[(2-hexadecanoylamino-3-hydroxyoctadec-4-ynyloxy)-hydroxylphosphoryloxy]ethyl}tri-methylammonium (tripleSM), which bears a triple bond linkage between C4–C5 (Fig. 1d). Because the triple bond linkage imposes the streight alignment on the C3–C6 carbons, the conformation of its hydrocarbon chain should be largely different from the other SMs. Furthermore, it is also expected that the comparisons of DHSM and tripleSM with eSM allow us to collect systematic data about the influence of bond order on membrane properties and their interaction with chol.

Density measurements revealed that tSM/chol and DHSM/chol bilayers show a chol-concentration dependent ordered phase formation similar to usual eSM/chol bilayers. TripleSM required a greater concentration of chol to completely transform the bilayer into the ordered phase, and the chol-induced condensation was smaller than that in the eSM/chol mixture. Moreover, the ordered phase formed in these SM/chol monolayers was characterized on the basis of the molecular areal compressional modulus C_{mol}^{-1}, which corresponds to the rigidity of an SM molecule in the SM/chol mixture. The C_{mol}^{-1} value of DHSM was greater than that of eSM in the presence of 30 or more mol% of chol (ordered phase), while their compressibility was similar in the absence of chol. These results suggest that the DHSM/chol mixture forms a more ordered membrane than the eSM/chol mixture does. In the absence of chol, the C_{mol}^{-1} value of tripleSM was 1.8-fold higher than that of eSM. The triple bond in tripleSM increases membrane rigidity even in the absence of chol, while preventing chol-induced condensation.

Materials and Methods

Materials

Erythro-sphingomyelin with a C18:0 hydrocarbon chain (eSM) was extracted from porcine brain derived SM by HPLC. Dihydrosphingomyelin (DHSM) was synthesized according to the procedure of Kan *et al*.[19]. *Threo*-sphingomyelin with a C18:0 hydrocarbon chain (tSM) and (2*S*,3*S*)-{2-[(2-hexadecanoylamino-3-hydroxyoctadec-4-ynyloxy)-hydroxyphosphoryloxy]ethyl}trimethylammonium (tripleSM) were synthesized according to Schemes 1a and b, respectively (see below and supplementary data). Cholesterol (chol) was purchased from Sigma Aldrich (St. Louis, MO). Other chemicals were purchased from Wako Pure Chemical Industries, Ltd. (Osaka, Japan). These lipids were dissolved in chloroform/methanol (4:1) at a concentration of 1 mg/mL and stored at ~5°C until use, unless otherwise mentioned.

Synthesis

Two of the SM analogues, tSM (1) and tripleSM (2), were prepared as shown in Scheme 1. For *threo*-derivative 1, Garner's aldehyde 3[20] was treated with 1-pentadecynyl lithium prepared from pentadec-1-yne and *n*-butyl lithium, in the presence of anhydrous $ZnBr_2$ to furnish the *threo*-alkynol 4 in a 60% yield with excellent diastereoselectivity[21] (Scheme 1A). After stereoselective reduction of the triple bond with Red-Al, PMB protection of the hydroxyl group and subsequent removal of the acetonide unit under acidic conditions afforded the primary alcohol 5. Then, the phosphocholine moiety was introduced into the hydroxyl group of 5 by a bromine-mediated one-pot procedure with moderate yield[22], followed by removal of the PMB and Boc groups with TFA and stearylation of the amino group to give the desired *threo*-SM 1 in a 66% yield. For triple-bond-derivative 2, the addition of 1-pentadecynyllithium to Garner's aldehyde 3 in THF afforded the *erythro*-alkynol 7 in a 87% yield with high diastereoselectivity[23] (Scheme 1B). From compound 7, the desired triple bonded SM 2 was obtained *via* the same four-step conversion as reactions c-f in Scheme 1A.

Differential Scanning Calorimetry (DSC).

The main transition temperatures of pure eSM, tSM, DHSM, and tripleSM bilayers were examined by DSC. Samples were prepared by a conventional method. Briefly, the appropriate amount of SM powder was dispersed in distilled water and incubated at 55°C for eSM, tSM, and DHSM, and at 65°C for tripleSM (temperatures higher than the main transition temperature of each sample) for 10 min with intermittent vortexing. Final lipid concentrations of the samples were 13 wt%. Then, 10–15 μL of the sample (1.3–2.0 mg lipid) was enclosed in an aluminum pane (0219-0062, Perkin Elmer, California) and placed into the DSC (Diamond, Perkin Elmer, California) immediately before measurements. The temperature was calibrated using representative phospholipid bilayers with established transition temperatures: DMPC (24.5°C), DPPC (41.5°C), and DSPG (53.5°C)[24]. A scanning rate of 5.0°C/min was used for all DSC measurements.

Density measurements

According to Nagle's group and others, the neutral floatation method allows estimation of the specific volume (inverse density) of a bilayer sample using H_2O/D_2O mixtures as a solvent[25–28]. Theoretically, the specific volumes of H_2O and D_2O are referred to as v_{H_2O} and v_{D_2O}, respectively. The specific volume of the solvent v_{sol} is defined as:

$$v_{sol} = \varphi v_{D_2O} + (1-\varphi) v_{H_2O},$$

where φ is the mass fraction of D_2O. If the specific volume of lipid vesicle (v) is larger than v_{sol}, the vesicle floats in the H_2O/D_2O solvent. If the value of v is smaller than v_{sol}, the vesicle sinks in the solvent. The floating/sinking process

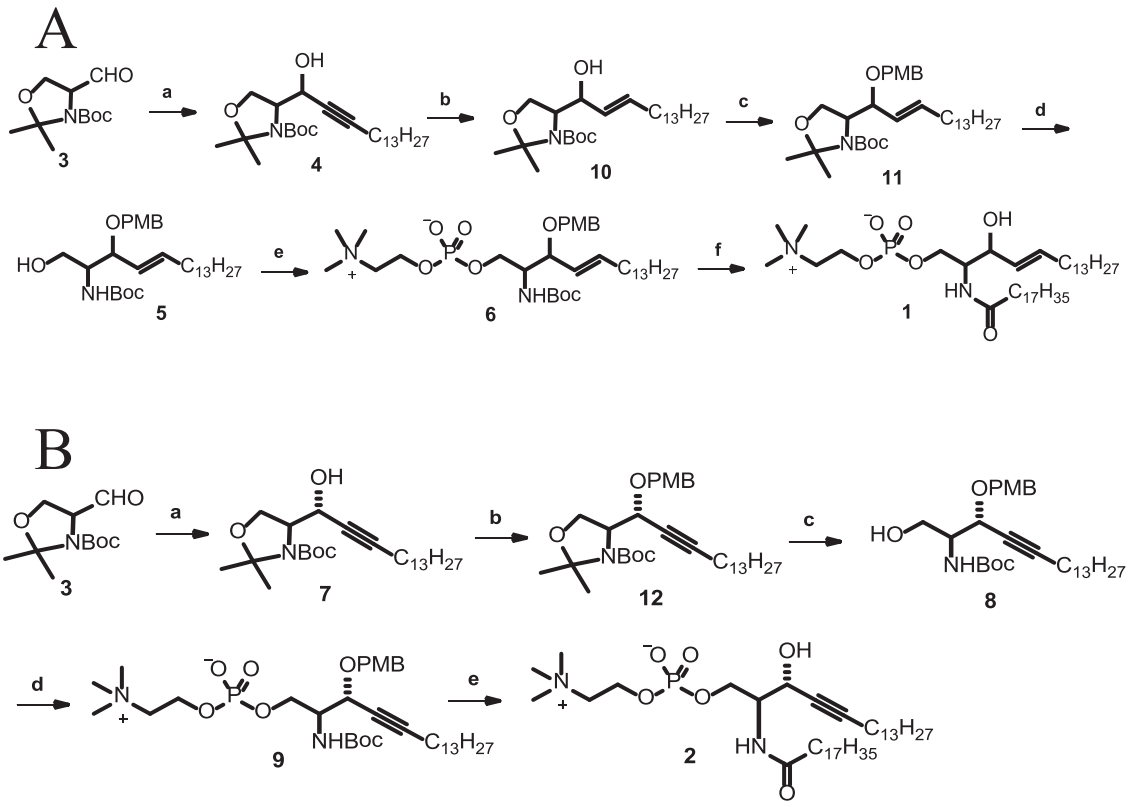

Scheme 1 (A) Reagents and conditions: a) *n*-BuLi pentadecyne, $ZnBr_2$, Et_2O, −78°C to rt, 20 h, 60%; b) RedAl, Tol, Et_2O, 0°C, 15 h, 100%; c) NaH, PMBCl, TBAI, THF, 0°C to rt, 20 h, 92%; d) LiCl, AcOH, H_2O, rt, 2 h, 59%; e) i) 2-chloro-1,3-dioxaphospholane, DIPEA, CH_2Cl_2, 0°C, 1 h, ii) bromine, 0°C, 10 min, iii) 30% aq. NMe_3, MeCN, *i*-PrOH, $CHCl_3$, 22 h, 44%; f) i) TFA, CH_2Cl_2, 0°C, 30 min, ii) 4-nitrophenyl stearate, Et_3N, DMPA, THF, rt, 23 h, 66%. (B) Reagents and conditions: a) *n*-BuLi pentadecyne, THF, −20°C, 5.5 h, 87%; b) NaH, PMBCl, TBAI, THF, 0°C to rt, 20 h, 99%; c) LiCl, AcOH, H_2O, rt, 3 h, 75%; d) i) 2-chloro-1,3-dioxaphospholane, DIPEA, CH_2Cl_2, 0°C, 1 h, ii) bromine, 0°C, 10 min, iii) 30% aq. NMe_3, MeCN, *i*-PrOH, $CHCl_3$, 20 h, 68%; e) i) TFA, CH_2Cl_2, 0°C, 1 h, ii) 4-nitrophenyl stearate, Et_3N, DMPA, THF, rt, 39 h, 38%.

can be facilitated by centrifugation. When the sample is obtained in the supernatant in a solvent with a specific volume of v_{sol}^{sup} and the precipitate is in a solvent with v_{sol}^{prep}, the specific volume of the sample (v) can be determined by:

$$v = \frac{v_{sol}^{sup} + v_{sol}^{prep}}{2} \pm \frac{v_{sol}^{sup} - v_{sol}^{prep}}{2}.$$

Here, the latter term corresponds to the measurement error.

Experimentally, the appropriate amount of SM and chol co-dissolved into a MeOH/$CHCl_3$ solution (1:4 v/v) was dried under a N_2 flow and stored under a vacuum for more than 24 h to remove all organic solvents. The dried sample was dispersed in H_2O/D_2O and incubated for several minutes at 50°C for eSM/chol and tSM/chol mixtures, at 55°C for the DHSM/chol mixture, and at 63°C for the tripleSM/chol mixture with intermittent vortexing. The final lipid concentration was ~5 mM. The incubated sample was rapidly transferred into the centrifuge (Kubota Model 1910, Kubota Co., Ltd., Tokyo, Japan) and centrifuged (20,000×*g*) for 5–20 min at 50°C for eSM/chol and tSM/chol mixtures, at 55°C for the DHSM/chol mixture, and at 63°C for the tripleSM/chol mixture. DSC measurements showed that all samples formed a fluid phase under these conditions. The temperature of the sample was measured directly using a K-type thermometer (AD-5602A, Sansyo Industries, Ltd., Tokyo, Japan) immediately after centrifugation. When the sample was reused, it was heated and cooled several times around the main transition temperature after the addition of H_2O or D_2O. Voids or packing defects are formed most intensively in lipid membranes around the transition temperature, resulting in a homogeneous v_{sol} value between the exterior and interior of a lipid vesicle[29]. The measurements were repeated 3 to 5 times under identical conditions to obtain reliable results.

Surface pressure vs. molecular area measurements

Monolayers of lipid mixtures were prepared on a computer-controlled Langmuir film balance (USI System, Fukuoka, Japan) calibrated using stearic acid. The subphase was distilled and freshly deionized water was obtained from a Milli-Q System (Millipore Corp., Tokyo, Japan). The apparatus was covered with vinyl sheets, which prevented deposition of dust on the water surface. A total of 30 μL of lipid solution (1 mg/mL) was spread onto the aqueous subphase

($100\times290\,mm^2$) with a glass micropipette (Drummond Scientific Company, Pennsylvania, USA). The monolayers were compressed at a rate of $10\,mm^2$/s after an initial delay period of 10 min for evaporation of organic solvents. The subphase temperature was controlled to 25.0±0.1°C. The measurements were repeated 3 to 5 times under the same conditions to obtain reliable results. These measurements provided the molecular area at the corresponding pressure within an error of ~±1 Å^2. The influence of oxidation on the unsaturated chains in SM was examined at the air-water interface by intentionally exposing pure SM monolayers to air for 10–30 min before compression[30]. The change in the isotherm after the prolonged exposure of SM molecules to air was within the error described above.

Analysis

Using the experimentally obtained specific volume (v) of components 1 and 2 (*e.g.*, SM and chol, respectively) in a binary sample, the mean molecular volume (v_{mean}) can be expressed as:

$$v_{mean}(x) = \frac{\{(1-x)M_1 + xM_2\}v(x)}{N_A}, \quad (1)$$

where M_1 and M_2 are the molecular weights of components 1 and 2, respectively, N_A is the Avogadro number, and x is the molar fraction of component 2. According to Greenwood *et al*., partial molecular volumes of components 1 V^1_{PMV} and 2 V^2_{PMV} can be defined as:

$$V^1_{PMV} = \left(\frac{\partial N v_{mean}}{\partial N_1}\right) \quad (2)$$

and

$$V^2_{PMV} = \left(\frac{\partial N v_{mean}}{\partial N_2}\right), \quad (3)$$

where N is the total amounts of components 1 and 2 (N_1 and N_2, respectively)[28]. On the basis of the additivity rule, the v_{mean} also can be expressed as:

$$v_{mean}(x) = (1-x)V^1_{PMV}(x) + xV^2_{PMV}(x). \quad (4)$$

Denoting derivatives with respect to x by prime yields, the following equations are obtained:

$$V^1_{PMV}(x) = v_{mean}(x) - xv'_{mean}(x) \quad (5)$$

and

$$V^2_{PMV}(x) = v_{mean}(x) + (1-x)v'_{mean}(x). \quad (6)$$

Using the experimentally obtained mean molecular area A_{mean}, as in the case for the estimation of the partial molecular volumes, the respective partial molecular areas of components 1 and 2 (A^1_{PMV} and A^2_{PMV}, respectively) can be expressed as:

$$A^1_{PMV}(x) = A_{mean}(x) - xA'_{mean}(x) \quad (7)$$

and

$$A^2_{PMV}(x) = A_{mean}(x) + (1-x)A'_{mean}(x), \quad (8)$$

where x is the molar fraction of component 2[31].

Areal compressibility (C_s) at a given surface pressure of π was calculated from the π-A isotherm using:

$$C_s = -\frac{1}{A_{mean}}\left(\frac{\partial A_{mean}}{\partial \pi}\right)_\pi, \quad (9)$$

where the A_{mean} is the experimentally obtained mean molecular area. The compressibility in ideal mixtures of components 1 and 2 (C_{12}) was calculated according to Alie *et al*.:

$$C_{12} = \left(\frac{1}{A_{12}}\right)\{(C_{s1}A_1)X_1 + (C_{s1}A_2)X_2\}, \quad (10)$$

where C_{s1} and C_{s2} are the compressibilities of pure components 1 and 2, respectively[32]. The results suggested that C_{12} is additive with respect to the product of C_{si} and A_i, rather than C_{si} for either ideal or completely non-ideal mixing. Compressibility (C_s) was expressed in terms of areal compressional modulus (C_s^{-1}) for easy comparison with previous data.

Results

The thermal phase behavior of pure eSM, tSM, DHSM, and tripleSM bilayers was investigated using calorimetric methods. In the DSC heating thermogram, pure eSM bilayers gave rise to a sharp peak corresponding to the chain melting (main) transition at 44.5°C as shown in Figure 2a. Therefore, the transition temperature (T_m), 43.5°C, of tSM bilayers is slightly lower than that of eSM bilayers (Fig. 2b); these T_m values are consistent with previous results[12]. In contrast, the respective T_m values of 50.0°C and 58.0°C for DHSM and tripleSM bilayers are significantly higher than that of eSM (Fig. 2c and d).

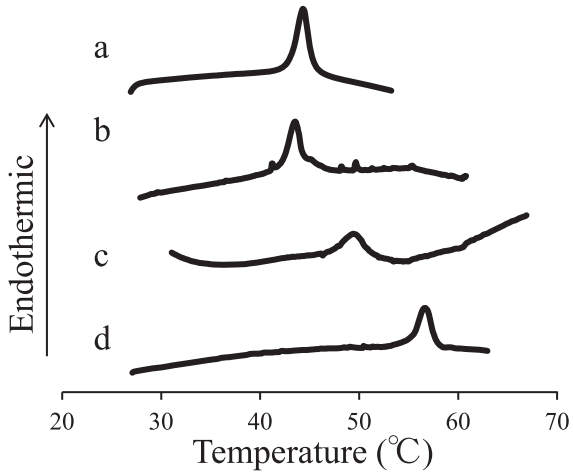

Figure 2 DSC 1st heating thermograms of (a) eSM, (b) tSM, (c) DHSM, and (d) tripleSM bilayers after sample preparation.

To evaluate the influence of chol on lipid packing in the fluid phase ($T>T_m$), the density of SM and chol mixtures was measured. Figure 3 shows the specific volumes (inverse density) (v) of SM/chol mixtures above T_m as a function of molar fractions of chol (x_{chol}).

In eSM/chol bilayers, the x_{chol}-dependence of v appeared to fit two linear functions; the value of v decreased as the molar fraction of x_{chol} increased and reached a plateau at $x_{chol}=0.25$ (Fig. 3a). The chol concentration, at which the decrease in v reached a plateau, is tentatively called the 'break point'. According to Greenwood *et al*., the chol-induced transition from disorder-to-order phase is completed at the break point[28]. The v values of the tSM/chol and DHSM/chol mixtures showed a similar x_{chol}-dependence to that of eSM/chol mixtures, in which the ordered phase formation was completed at $x_{chol}=0.25$ (Fig. 3b and c). The value of v for the tripleSM/chol mixture revealed a different x_{chol}-dependence; its breakpoint ($x_{chol}=0.40$) was significantly higher than that of the other SM/chol mixtures (Fig. 3d). Therefore, greater concentrations of chol were needed for tripleSM to complete the formation of the ordered phase. Under the present conditions, the value of v for pure SM bilayers could not be determined because a value that is greater than that of H_2O in the fluid phase causes floating of the membrane preparations.

From experimentally obtained v values, the mean molecular volume (v_{mean}) was calculated using Eq. (1), which was plotted as a function of x_{chol} (Fig. 4). The data in Figure 4 were fitted by two linear functions, which crossed each other at the break point (see Fig. 3). The intersection between each linear function and $x_{chol}=0$ corresponded to the partial molecular volume of SM (V_{PMV}^{SM}), while the intersection between each linear function and $x_{chol}=1$ corresponded to the partial molecular volume of chol (V_{PMV}^{chol}) according to Eqs. (5) and (6). The V_{PMV}^{SM} and V_{PMV}^{chol} values were defined as the increase in volume resulting from the addition of one SM molecule or one chol molecule, respectively, at a given x_{chol} (see Eqs. (2) and (3)).

The partial molecular volumes of SM and chol were plotted as a function of x_{chol} (Fig. 5a and b, respectively). A decrease in partial molecular volume of eSM at the break point ($x_{chol}=0.25$) shows the completion of the ordered phase formation (circles in Fig. 5a). In the tSM/chol and DHSM/chol mixtures, the partial molecular volume of each SM showed a similar biphasic response; the partial molecular volumes of tSMand DHSM decreased at $x_{chol}=0.25$. In contrast, the tripleSM/chol bilayers showed a higher break point ($x_{chol}=0.40$) than the other SM/chol mixtures. However, in this analysis, the decrease in a V_{PMV}^{SM} value at the break point must cause the underestimation of the chol-induced condensation of an SM molecule, because an added SM molecule does not necessarily directly contact chol, especially at lower concentrations of chol. Thus, the chol-induced condensation effect was estimated on the basis of the partial molecular volume of chol.

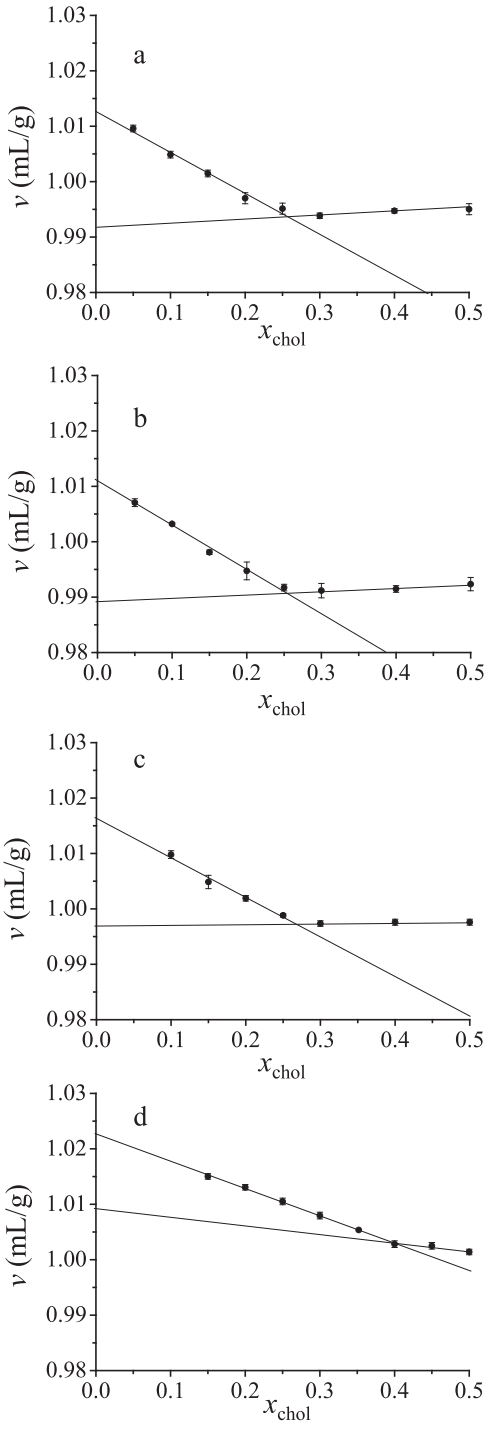

Figure 3 Specific volume (v) of (a) eSM/chol, (b) tSM/chol, (c) DHSM/chol, and (d) tripleSM/chol bilayers as a function of x_{chol}. Measurements were performed at 50°C for (a) and (b), at 55°C for (c), and 63°C for (d). Under these conditions, all samples formed the fluid phase. Data for each mixture were fitted to two linear functions (solid lines).

The V_{PMV}^{chol} value accounts not only for the volume of chol, but also for its effects on neighboring lipids, and thus the V_{PMV}^{chol} value includes condensation of neighbor lipids by

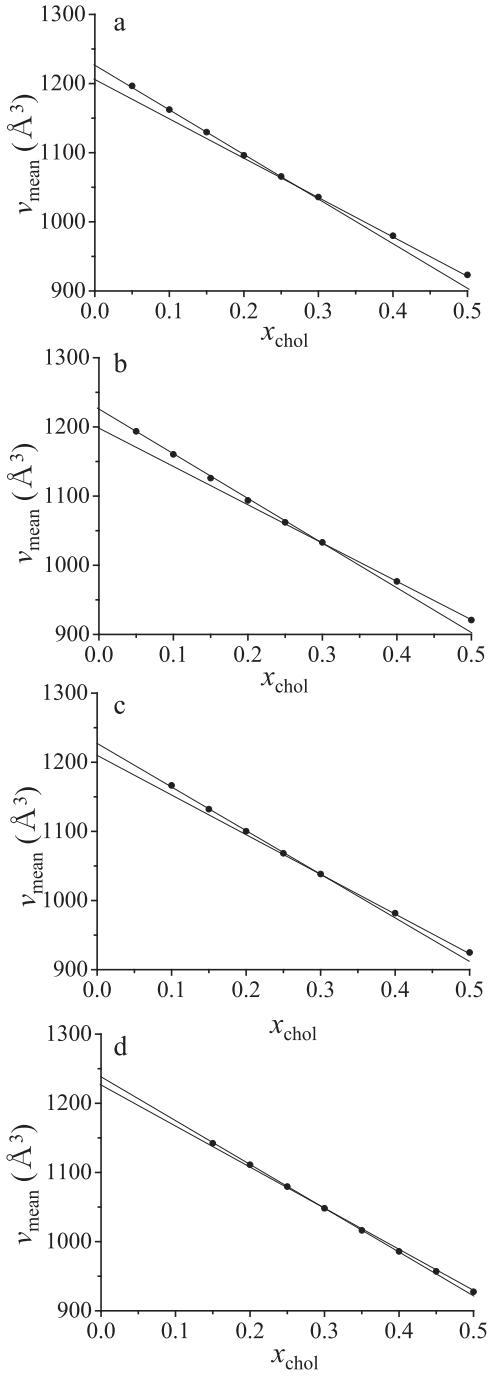

Figure 4 Mean molecular volume (v_{mean}) of (a) eSM/chol, (b) tSM/chol, (c) DHSM/chol, and (d) tripleSM/chol mixtures as a function of x_{chol}. The v_{mean} was calculated from v as shown in Figure 3 according to Eq. (1), and the data were fitted to two linear functions (solid lines).

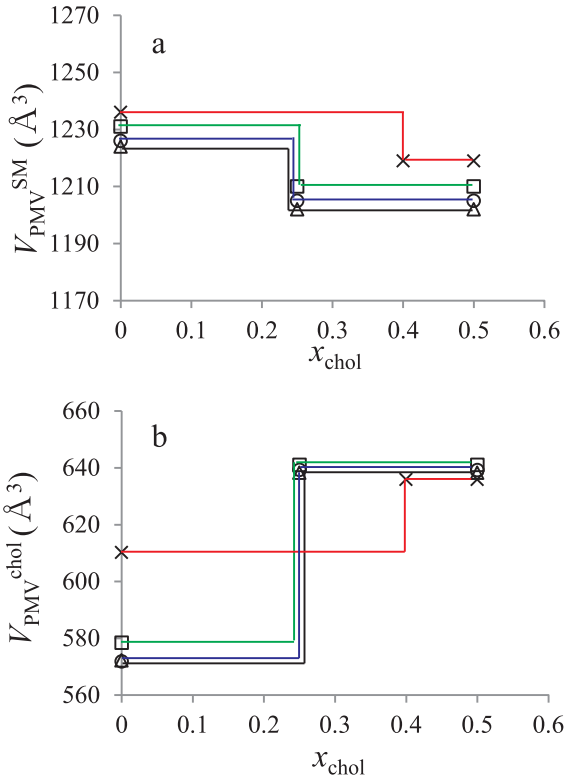

Figure 5 (a) Partial molecular volume (V_{PMV}^{SM}) of eSM (circles), tSM (triangles), DHSM (squares), and tripleSM (crosses) as a function of x_{chol}; (b) partial molecular volume of chol (V_{PMV}^{chol}) in eSM/chol (circles), tSM/chol (triangles), DHSM/chol (squares), and tripleSM/chol (crosses) mixtures as a function of x_{chol}. Partial molecular volumes were calculated using Eqs. (5) and (6).

chol[28]. Under lower concentrations of chol, the V_{PMV}^{chol} value is estimated to be 575±10 Å^3 for eSM/chol, tSM/chol, and DHSM/chol mixtures (Fig. 5b). In addition, the V_{PMV}^{chol} value for the tripleSM/chol mixture (610±5 Å^3) was larger than those for the other preparations. These results indicate that chol-induced condensation occurs in the tripleSM/chol mixture to a lesser extent than in the other SM/chol mixtures below the break point. In all the SM/chol mixtures, the V_{PMV}^{chol} values increased at each break point and became constant at approximately 638±5 Å^3 in the higher x_{chol} region. Previously, the value of 630±10 Å^3 was considered most appropriate for the volume of a bare chol molecule on the basis of partial molecular volume measurements[28]. Thus, the results we obtained indicate that further condensation of SM molecules by chol does not occur above a break point.

The surface pressure vs. molecular area isotherm (π-A isotherm) measurement gives direct information on the cross-sectional area of a lipid molecule at a given pressure. Figure 6 shows the π-A isotherms of eSM, tSM, DHSM, and tripleSM monolayers in the presence and absence of chol at 25°C. The pure eSM and tSM monolayers exhibited a transition from the liquid expanded (LE) phase to the liquid condensed (LC) phase at 10–20 mN/m (black lines in Fig. 6a and b). The transition pressure of pure DHSM monolayers (5–12 mN/m) was less than that of eSM. Thus, the LC phase is more stable in the DHSM monolayer than in the eSM monolayer (black line in Fig. 6c). In addition, the tripleSM monolayer showed no transition, and judged from the membrane rigidity, the tripleSM monolayer is thought to

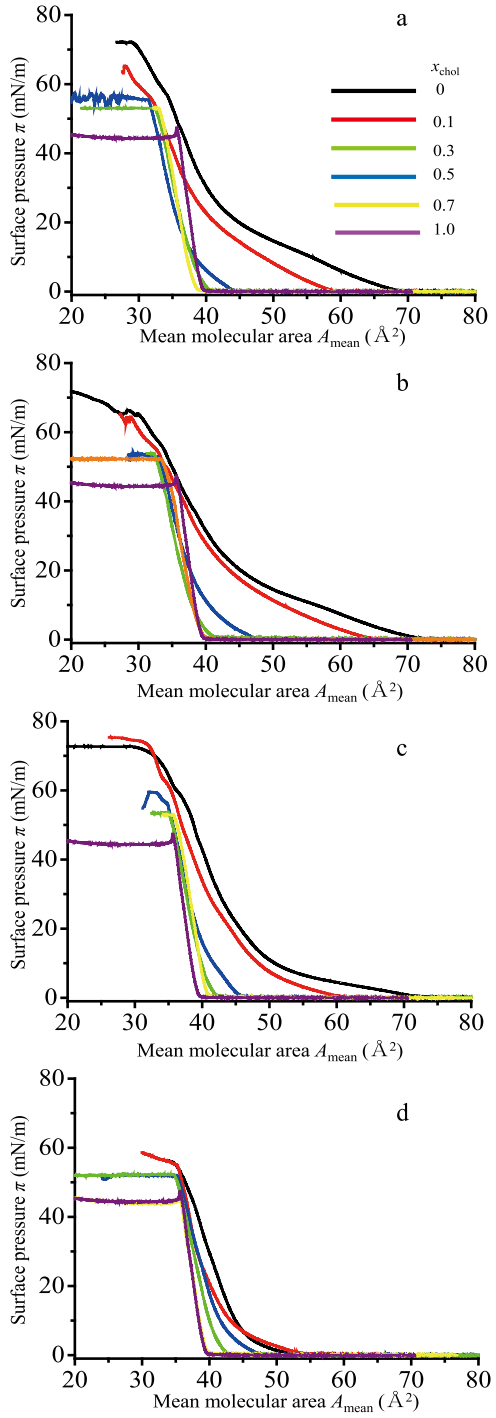

Figure 6 Surface pressure vs. molecular area isotherms of (a) eSM/chol, (b) tSM/chol, (c) DHSM/chol, and (d) tripleSM/chol mixtures at 25°C. x_{chol} is directly described in the figure.

form a homogeneous ordered phase throughout the entire experimental pressure range (see below).

On the basis of π-A isotherms, the mean molecular areas A_{mean} of SM/chol mixtures at a physiological relevant pressure (30 mN/m) were plotted as a function of x_{chol}[33–36]. The A_{mean} value of the eSM/chol mixture decreased as the x_{chol} value increased and reached a plateau at x_{chol}=0.30 (Fig. 7a). The A_{mean} value of tSM/chol and DHSM/chol mixtures showed a similar dependence on x_{chol} (Fig. 7b and c). On the other hand, in the tripleSM/chol mixtures, the A_{mean} decreased monotonously as the x_{chol} value was increased.

On the basis of the A_{mean} data, the partial molecular areas (A_{PMA}^{SM}) of eSM, tSM, DHSM, and tripleSM, and those of chol A_{PMA}^{chol} in these SM/chol mixtures, were estimated as was the case with the partial molecular volumes (Eqs. (7) and (8)). These A_{PMA}^{SM} and A_{PMA}^{chol} values corresponded to the lateral area expansion by the addition of one SM molecule and one chol molecule, respectively. In the eSM/chol, tSM/chol, and DHSM/chol mixtures, the break point (decrease in A_{PMA}^{SM} value) appeared at x_{chol}=0.30. The break point obtained in these SM/chol monolayer systems is somewhat close to that obtained in bilayer systems (x_c=0.25, see Fig. 5). In contrast, the A_{PMA}^{SM} value of tripleSM is constant regardless of x_{chol}, and no break point appears, showing that the chol-induced phase transition does not occur in tripleSM/chol monolayers.

The chol-induced condensation of SM could be evaluated from the A_{PMA}^{chol} for each SM/chol mixture as in the case for the density measurements. Under the lower x_{chol} region, the A_{PMA}^{chol} of the eSM/chol mixture was estimated to be 23 Å^2, which was relatively close to those of the tSM/chol and DHSM/chol mixtures (24 Å^2 and 27 Å^2, respectively). Therefore, the chol-induced lateral condensation of tSM and DHSM is similar to that of eSM. However, in the tripleSM/chol monolayers, no break point appears and the A_{PMA}^{chol} value of 36 Å^2 is constant irrespective of x_{chol}. Because this value is consistent with the cross-sectional area of a pure chol at a given pressure of 30 mN/m, tripleSM is not condensed by chol in the experimental x_{chol} range.

Previously, Li *et al*. reported that the liquid ordered phase brings forth a notable decrease in the membrane elasticity[37]. Here, we examined the phase behavior of each SM/chol monolayer on the basis of membrane rigidity and qualitatively characterized the ordered phase formed in each SM/chol mixture. According to Eq. (9), the slope of the π-A isotherm shows the areal compressional modulus (C_s^{-1}); thus, the C_s^{-1} values at 30 mN/m were plotted as a function of x_{chol} (Fig. 9). The solid lines show the ideal behavior of C_s^{-1} in each SM/chol mixture (Eq. (10)). The C_s^{-1} values of the eSM/chol, tSM/chol, and DHSM/chol mixtures behave ideally only at lower chol-concentrations ($x_{chol}\leq$0.10). A further increase in the x_{chol} value led to a deviation in C_s^{-1} values from the ideal line. Because these SM/chol mixtures form the homogeneous ordered phase above a break point (x_{chol}=0.30), the molecular areal compressional modulus of each SM C_{mol}^{-1} in the ordered phase was estimated by fitting the C_s^{-1} data in the $x_{chol}\geq$0.30 region to Eq. (10) (dashed lines in Fig. 9). Namely, the intersectional value of the dashed line at x_{chol}=0 corresponds to the C_{mol}^{-1} of SM in the ordered phase, and that of the solid line at x_{chol}=0 corresponds to the C_{mol}^{-1} of SM in the LC phase. The estimated

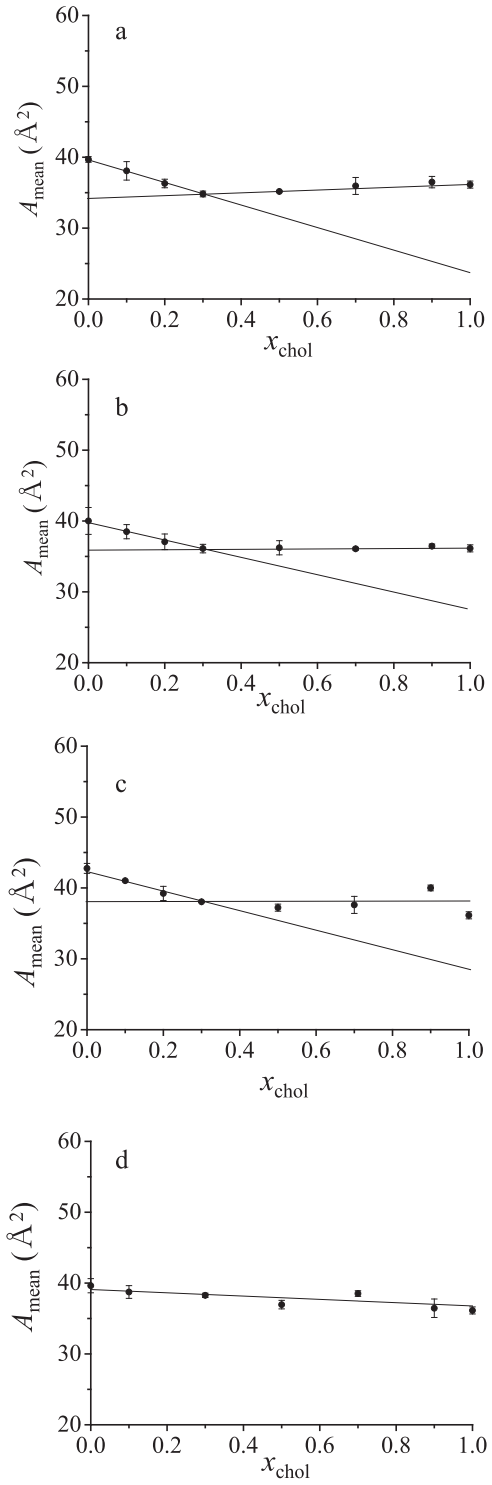

Figure 7 Mean molecular area (A_{mean}) of (a) eSM/chol, (b) tSM/chol, (c) DHSM/chol, and (d) tripleSM/chol monolayers as a function of x_{chol} at 30 mN/m. The data were fitted to two linear functions except for (d) (solid lines).

C_{mol}^{-1} values for each SM in the LC phase and the ordered phase are summarized in Table 1. The C_{mol}^{-1} value of 140 mN/m of eSM in the LC phase increased to 240 mN/m in the ordered phase. The respective C_{mol}^{-1} values of 120 mN/m and 220 mN/m of tSM indicated similar rigidity to that of eSM both in the LC phase and the ordered phase. The C_{mol}^{-1} value of DHSM (290 mN/m) was greater than that of eSM in the ordered phase, although the C_{mol}^{-1} value of DHSM was similar to that of eSM in the LC phase. These results indicate that DHSM interacts more favorably with chol than eSM does. However, the C_{mol}^{-1} value of 250 mN/m of tripleSM appears to be constant throughout the experimental x_{chol} range. This result is consistent with the areal analysis results; the chol-induced condensation does not occur in tripleSM/chol mixtures (Fig. 8). Considering that the C_{mol}^{-1} value of tripleSM (250 mN/m) is similar to that of eSM in the ordered phase (240 mN/m), the properties of a pure tripleSM monolayer may be similar to those of eSM/chol monolayers in the ordered phase.

We also estimated the C_{mol}^{-1} value of each SM analogues at 5 mN/m and found that the influence of chol on the SM rigidity is largely similar between 5 mN/m and the 30 mN/m (supplementary Table S1 and Fig. S1). Briefly, the C_{mol}^{-1} value of tSM is similar to that of eSM both below (40 mN/m and 50 mN/m, respectively) and above each break point (110 mN/m and 120 mN/m, respectively). The C_{mol}^{-1} value of DHSM (150 mN/m) was greater than that of eSM (120 mN/m) above each break point. Accompanied by the phase transition, an increase in the C_{mol}^{-1} value is smaller for the tirpleSM (+40 mN/m) than the eSM (+70 mN/m). On the other hand, in those mixtures except for tripleSM/chol, the break points obtained at 5 mN/m (x_{chol}=0.40–0.50) are about 2 fold higher than that obtained in the bilayer systems (x_{chol}=0.25), showing that the x_{chol}-dependent phase behavior at 30 mN/m obtained in the monolayer systems is similar to that obtained in the bilayer systems because the break points obtained at 30 mN/m (x_{chol}=0.30) are closer to those obtained in bilayers systems. Thus, we preferentially focus on the C_{mol}^{-1} value at 30 mN/m rather than that at 5 mN/m below.

Discussion

To obtain basic information on the properties of membranes comprised of eSM, tSM, DHSM, and tripleSM, the thermal phase behavior of these bilayers was examined by calorimetry. The DSC measurements showed that T_m of a pure tSM bilayer was slightly lower than that of a pure eSM bilayer (Fig. 2). Previously, Bruzik suggested that the conformation of the C1–C2 bond of a sphingosine moiety in eSM is restricted, while the same bond in tSM can easily rotate in the gel phase[13]. Therefore, the conformational stability of eSM in the gel phase results in a slightly higher T_m of its bilayer. However, the influence of conformational motion on lipid packing must be small as compared to the influence of bond order at the interfacial region, because the T_m values of DHSM and tripleSM bilayers are much higher than that of an eSM bilayer. It is speculated that, in the gel

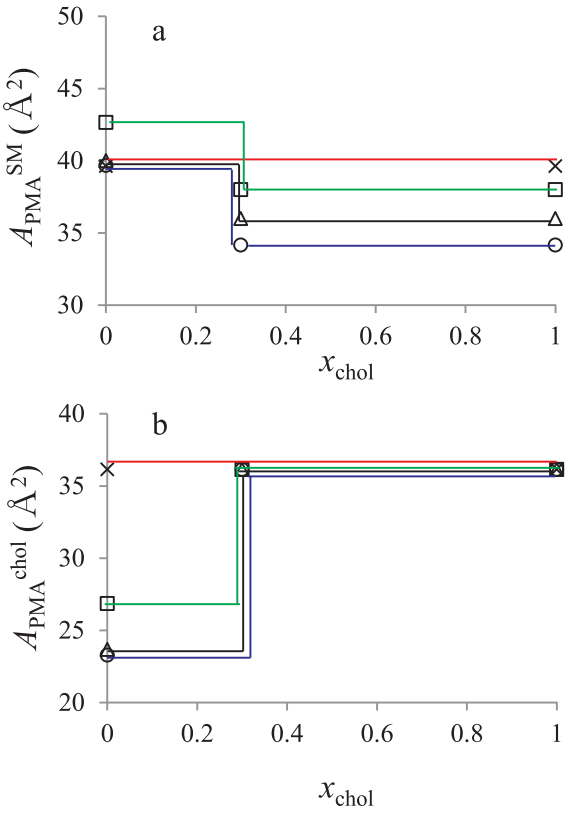

Figure 8 (a) Partial molecular area (A_{PMA}^{SM}) of eSM (circles), tSM (triangles), DHSM (squares), and tripleSM (crosses) as a function of x_{chol}. (b) Partial molecular area (A_{PMA}^{chol}) of chol in eSM/chol (circles), tSM/chol (triangles), DHSM/chol (squares), and tripleSM/chol (crosses) monolayers as a function of x_{chol}. Partial molecular volumes were calculated using Eqs. (7) and (8).

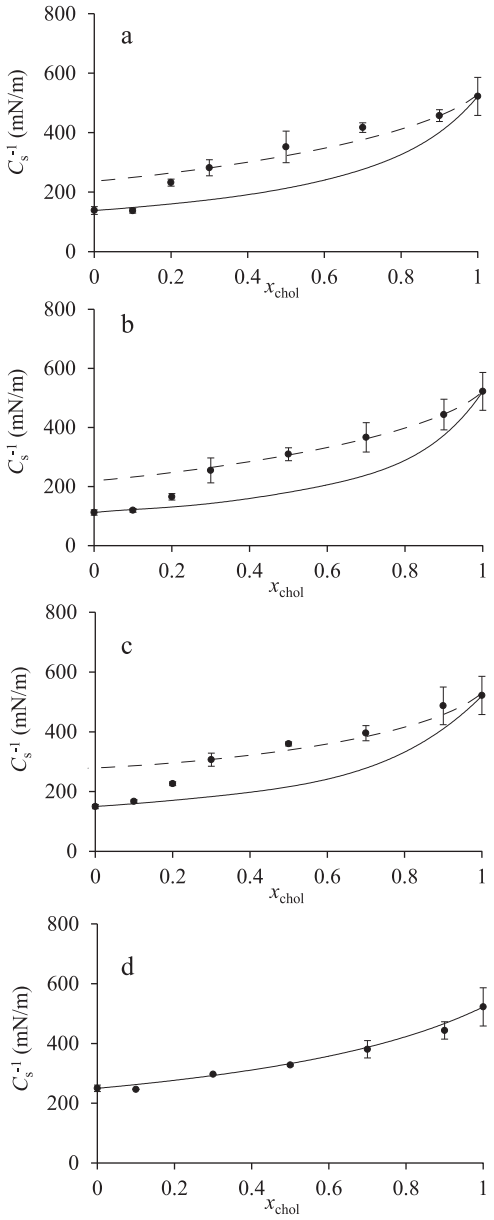

Figure 9 Areal compressional modulus (C_s^{-1}) of (a) eSM/chol, (b) tSM/chol, (c) DHSM/chol, and(d) tripleSM/chol monolayers as a function of x_{chol}. Solid lines indicate the ideal C_s^{-1} as expressed by Eq. (10). Dashed lines indicate fit of the data above the break point to Eq. (10), while regarding C_s^{-1} of SM as a variable. The intersection between the dashed line and $x_{chol}=0$ corresponds to the rigidity of SM in the ordered phase (C_{mol}^{-1}). Here, the break point used was estimated by Figure 8.

phase, the alkyl chains in DHSM and tripleSM bilayers are more tightly packed than those in eSM and tSM bilayers.

Above main transition temperature, we examined the chol-induced ordered phase formation of the SM/chol mixtures using several techniques. The density measurements and the π-A isotherm experiments revealed that the tSM/chol mixture exhibits a x_{chol}-dependent phase behavior similar to that of the eSM/chol mixture; the chol-induced disordered-to-ordered phase transition was completed at $x_{chol}=0.25$ in the bilayer and $x_{chol}=0.30$ in the monolayer (Fig. 5 and 8, respectively). Previous steady-state anisotropy measurements showed that the ordered phase formation of eSM/chol bilayers is completed at $x_{chol}\sim0.3$ at 50°C[38]. In addition, the DSC measurements also showed that the endothermic peak corresponding to the main transition of pure C16:0-eSM domains disappears in the presence of 25–30 mol% chol[39]. These results imply that the break point obtained through the present measurements ($x_{chol}=0.25$–0.30) is reliable, and that the data obtained in monolayer systems are largely consistent with those obtained in bilayer systems. Previous density measurements showed the break point of the DPPC/chol binary bilayer at $x_{chol}=0.27$[28], which is similar to that of eSM/chol binary bilayers ($x_{chol}=0.25$) obtained in the present work. These results indicate that DPPC has a similar capacity of chol to that of eSM. However, we should not directly compare the data obtained in C18:0-eSM/chol with those in DPPC (diC16:0-PC)/chol because the chain length of the lipid may affects the break point. In order to evaluate the difference in the chol-affinity between SM and PC, a further study using distearoylphosphatidycholine (diC18:0-

Table 1 Molecular areal compressional modulus (C_{mol}^{-1}) of each SM in the LC phase ($x_{chol} = 0$) and the ordered phase ($x_{chol} > 0.3$) at 30 mN/m

	$x_{chol}=0$ (LC phase)	$x_{chol}>0.3$ (ordered phase)
eSM/chol	140 mN/m	240
tSM/chol	120	220
DHSM/chol	150	290
tripleSM/chol	250*	

* The C_{mol}^{-1} value of tripleSM seems to be constant over all the x_{chol} range

PC)/chol mixtures will be necessary.

Partial molecular volume/area analysis showed similar chol-induced condensation effects between eSM and tSM; in other words, the V_{PMV}^{chol} and A_{PMA}^{chol} values for tSM are similar to those for eSM, and the chol-induced condensation effect for tSM is very similar to that for eSM (Fig. 5 and 8, respectively). Moreover, π-A isotherm measurements showed that eSM and tSM give rise to similar C_{mol}^{-1} values both in the LC and the ordered phases (Table 1). Probably because the carbon chains of the SM molecules melt and are disordered both in the fluid phase and the LC phase, the influence of the stereoconfiguration of the hydroxyl group at C3 may be hidden in the mobility of the hydrocarbon chain and does not have a major influence on the SM-chol interaction.

Why does eSM naturally occur but not tSM? In biological systems, the hydrolysis of SM molecules by sphingomyelinase produces phosphocholine and ceramide. The latter product is involved in cell differentiation[40], regulation of cell growth[41], apoptosis[42], and so on. Previously, it was reported that the activity of ceramide depends on its stereoconfiguration; *i.e.* D-*erythro*-ceramide (eCer) shows more moderate inhibition of cell growth than L-*threo*-ceramide[41]. Although it is not clear why the moderate activity of eCer is necessary for the regulation of cell growth, differences in the activity of the breakdown products is a possible explanation for the stereo-selective biosynthesis of eSM.

The density and π-A isotherm measurements demonstrated that the x_{chol}-dependent phase behavior of a DHSM/chol mixture is similar to that of an eSM/chol mixture; these mixtures have the same break point at $x_{chol}=0.3$ in a monolayer system and $x_{chol}=0.25$ in a bilayer system (circles and triangles in Fig. 5 and 8, respectively). Using DSC measurements, Nyholm *et al*. showed that the addition of chol into a C16:0-DHSM bilayer gives rise to a new transition peak at the higher temperature side of the main transition, and suggested that the new peak corresponds to the chain melting of the chol-rich ordered domain[18]. In their measurements, the main transition enthalpy of C16:0-DHSM bilayers (ΔH= 35.4 kJ/mol) decreased as the x_{chol} value increased and reached 1.4 kJ/mol at $x_{chol}=0.25$. This result suggests that 96% of all DHSM bilayers are composed of the ordered phase at $x_{chol}=0.25$. On the other hand, the main transition of C16:0-eSM bilayers completely disappeared at $x_{chol}=0.25$ and all domains form the chol-rich phase under these conditions. Considering the previous results, the break point of the DHSM/chol mixture must be slightly higher than that of the eSM/chol mixture. Unfortunately, the difference in the break point between eSM/chol and DHSM/chol is too small to be detected by our technique. Interestingly, DHSM showed greater molecular rigidity, C_{mol}^{-1} (290 mN/m), than eSM (240 mN/m) in the ordered phase, while the difference was not great (150 mN/m and 138 mN/m, respectively) in the chol-absent LC phase (Table 1). If the capacity of chol is higher in a DHSM monolayer than that in a eSM monolayer as suggested previously, it is reasonable that DHSM is more rigid than eSM in the ordered phase.

As described in the first paragraph, the human lens membrane contains a larger amount of DHSM and chol than any other tissues. The high capacity of chol in the DHSM membrane is thought to be necessary to form rigid elongated cells such as fiber cells or lens fibers[43,44]. Previously, Rosenfeld and Spector reported that generalized 'decomposition' of lens fiber cells occurs with cataract formation[43]. In addition, Cenedella reported that the inhibition of chol biosynthesis is associated with cataract formation[44], indicating that a decrease in the concentration of chol results in cataract formation. It is speculated that the high capacity of chol in the DHSM membrane keeps the chol concentration high enough to constitute a rigid cellular membrane and, consequently, prevents the decomposition of fiber cells.

The tripleSM/chol bilayer showed a greater break point ($x_{chol}=0.40$) than the eSM/chol bilayer ($x_{chol}=0.25$). In addition, the chol-induced condensation of tripleSM is less than that of eSM; an increase in the V_{PMV}^{chol} value for tripleSM/chol mixtures at the break point is approximately 50% of that in eSM/chol mixtures (Fig. 5). The extended alignment of C3–C6 in the sphingosine backbone may cause steric hindrance when tripleSM approaches chol. In addition, this steric mismatch may attenuate the electrostatic interaction, *e.g*. hydrogen bonding between tripleSM and chol. It is speculative that steric mismatching and attenuation of the electrostatic interaction between tripleSM and chol must be the reason for the decrease in chol-induced condensation and, consequently, a greater concentration of chol is needed for carbon chain ordering. This idea could be supported by monolayer measurements. The π-A isotherm measurements showed a higher areal compressional modulus, C_s^{-1}, for tripleSM (250 mN/m) than that for eSM (140 mN/m) in the absence of chol (Table 1 and Fig. 9 a and d). The triple bond at C4–C5 moiety imposes on the straight alignment of carbons in the vicinity of the triple bond and, speculatively, the straight alignment of carbons (C3–C6) largely modulates the conformation of the carbon chains. Most likely, tripleSM molecules laterally contact around the position of the rigid triple bond, giving rise to a greater lateral compressional modulus. On the other hand, in the cases of the eSM monolayer, hydrocarbon chains may contact at the deeper region and the position around the double bond (C4–C5) does not contribute the lateral contact. If it is the case, the rigidity of

double bond does not affect the areal compressional modulus, resulting in the lower C_{mol}^{-1} value for the eSM monolayer. Moreover, in the presence of chol, tripleSM may also contact with chol at the rigid regions because chol-induced ordering and/or the ordered phase formation was not observed. However, complete information on the conformation of the carbon chains in tripleSM is unavailable; therefore, further study on the molecular structure of tripleSM is needed to explain the higher break point of the tripleSM/chol mixture.

Conclusion

In the present study, we examined the chol-concentration (x_{chol}) dependence of the ordered phase formation employing the usual eSM and three SM analogues. Moreover, using π-A isotherm measurements, we presented a new analysis to estimate the molecular rigidity of SM (C_{mol}^{-1}) in the SM/chol mixture and qualitatively characterized the ordered phase on the basis of the C_{mol}^{-1} value. Both in the monolayer and bilayer systems, eSM/chol and tSM/chol mixtures showed a similar x_{chol}-dependent phase behavior, and their membrane properties were also similar both in the disordered and ordered phases. The DHSM/chol mixture also showed a x_{chol}-dependence in the ordered phase formation similar to the eSM/chol mixture. On the other hand, the π-A isotherm measurements demonstrated a higher C_{mol}^{-1} value for DHSM than for eSM in the ordered phase ($x_{chol}>30$ mol%), indicating that DHSM has a higher capacity of chol than eSM does. Density measurements demonstrated that ordered phase formation in tripleSM/chol bilayers completes at $x_{chol}=0.40$, which is higher than that obtained in the eSM/chol bilayers. The partial molecular volume of chol (V_{PMV}^{chol}) in tripleSM/chol was larger than that in eSM/chol mixtures below break point. Because the V_{PMV}^{chol} value includes not only the bare volume of chol but also condensation of neighboring lipids, this result shows that the chol-induced condensation is smaller for tripleSM than for eSM. Moreover, considering that the C_{mol}^{-1} value of tripleSM in the absence of chol is as large as that of eSM in the ordered phase, tripleSM may form the ordered phase even in the absence of chol.

Acknowledgements

This work was carried out by JST ERATO, Lipid Active Structure Project.

References

1. Simons, K. & Ikonen, E. Functional rafts in cell membranes. *Nature* **387**, 569–572 (1997).
2. Huang, J. & Feigenson, G. W. A microscopic interaction model of maximum solubility of cholesterol in lipid bilayers. *Biophys. J.* **76**, 2142–2157 (1999).
3. Edidin, M. The state of lipid rafts: From model membranes to cells. *Annu. Rev. Biophys. Biomol. Struct.* **32**, 257–283 (2003).
4. Simons, K. & Vaz, W. L. Model systems, lipid rafts, and cell membranes. *Annu. Rev. Biophys. Biomol. Struct.* **33**, 269–295 (2004).
5. Barenholz, Y. Sphingomyelin-lecithin balance in membranes: composition, structure, and function relationships. in Physiology of Membrane Fluidity. (Schinitzky M. ed.) pp. 131–173 (CRC Press, Boca Raton, 1984.)
6. Harder, T. & Simons, K. Caveolae, DIGs, and the dynamics of sphingolipid-cholesterol microdomains. *Curr. Opin. Cell Biol.* **9**, 534–542 (1997).
7. Munro, S. Lipid rafts: elusive or illusive? *Cell* **115**, 377–388 (2003).
8. McMullen, T. P. W., Lewis, R. N. H. & McElhaney, R. N. Cholesterol-phospholipid interactions, the liquid-ordered phase and lipid rafts in model and biological membranes. *Curr. Opin. Coll. Int. Sci.* **8**, 459–468 (2004).
9. Silvius, J. R. Role of cholesterol in lipid raft formation: lessons from lipid model system, *Biochim. Biophys. Acta* **1610**, 174–183 (2003).
10. Ramstedt, B. & Slotte, J. P. Membrane properties of sphingomyelins. *FEBS Lett.* **531**, 33–37 (2002).
11. Kirat, K. E. & Morandat, S. Cholesterol modulation of membrane resistance to Triton X-100 explored by atomic force microscopy. *Biochim. Biophys. Acta* **1768**, 2300–2309 (2007).
12. Bruzik, K. S. & Tsai, M. D. A calorimetric study of the thermotropic behavior of pure sphingomyelin diasteromer. *Biochemistry* **26**, 5364–5368 (1987).
13. Bruzik, K. S. Conformation of the polar headgroup of sphingomyelin and its analogues, *Biochim. Biophys. Acta* **939**, 315–326 (1988).
14. Ramstedt, B., Leppimaki, P., Axberg, M. & Slotte, J. P. Analysis of natural and synthetic sphingomyelin using high performance thin-layer chromatography. *Eur. J. Biochem.* **266**, 997–1002 (1999).
15. Byrdwell, W. C. & Borchman, D. Liquid chromatography/mass-spectrometric characterization of sphingomyelin and dihydrosphingomyelin of human lens membranes. *Ophthalmic Res.* **29**, 191–206 (1997).
16. Kuikka, M., Ramstedt, B., Ohvo-Rekilä, H., Tuuf, J. & Slotte, J. P. Membrane properties of D-erytho-N-acyl sphingomyelin and their corresponding species. *Biophys. J.* **80**, 2327–2337 (2001).
17. Vieira, C. R., Munoz-Olaya, J. M., Sot, J., Jiménez-Baranda, S., Izquierdo-Useros, N., Abad, J. L., Apellániz, B., Delgado, R., Martinez-Picado, J., Alonso, A., Casas, J., Nieva. J. L., Fabriás, G., Mañes, S. & Goñi, F. M. Dihydrosphingomyelin impairs HIV-1 infection by rigidifying liquid-ordered membrane domains. *Chem. Biol.* **17**, 766–775 (2010).
18. Nyholm, T. K. M., Nylund, M. & Slotte, J. P. A calorimetric study of binary mixtures of dihydrosphingomyelin and sterols, sphingomyelin or phosphatidylcholine. *Biophys. J.* **84**, 3138–3146 (2003).
19. Kan, C. C., Ruan, Z. S. & Bittman, R. Interaction of cholesterol with sphingomyelin in bilayers membranes: Evidence that the hydroxyl group of sphingomyelin does not modulate the rate of cholesterol exchange between vesicles. *Biochemistry* **30**, 7759–7766 (1991).
20. Garner, P. & Park, J. M. J. The synthesis and configurational stability of differentially protected β-hydroxy-α-amino aldehydes. *J. Org. Chem.* **52**, 2361–2364 (1987).
21. Herold, P. Synthesis of D-*erythro*- and D-*threo*-sphingosine derivatives from L-Serine. *Helv. Chim. Acta* **71**, 354–362 (1988).
22. Erukulla, R. K., Byun, H.-S. & Bittman, R. Antitumor phospholipids: A one-pot introduction of a phosphocholine moiety into lipid hydroxy acceptors. *Tetrahedron Lett.* **35**, 5783–5784 (1994).

23. Blot, V., Jacquemard, U., Reissig, H.-U. & Kleuser, B. Practical Syntheses of Sphingosine-1-Phosphate and Analogues. *Synthesis* **5**, 759–766 (2009).
24. Caffrey, M. *LIPIDAT: A database thermodynamic data and associated information on lipid mesomorphic and polymorphic transitions*. (CRC press, Boca Raton, FL, 1993.)
25. Nagle, J. F., & Wilkinson, D. A. Lecithin bilayers-density measurements and molecular interactions. *Biophys. J.* **23**, 159–175 (1978).
26. Wiener, M. C., Tristram-Nagle, S., Wilkinson, D. A., Campbell, L. E. & Nagle, J. F. Specific volumes of lipids in fully hydrated bilayer dispersions. *Biochim. Biophys. Acta* **938**, 135–142 (1998).
27. Koenig, B. W. & Gawrisch, K. Specific volumes of unsaturated phosphatidylcholines in the liquid crystalline lamellar phase. *Biochim. Biophys. Acta* **1715**, 65–70 (2005).
28. Greenwood, A. I., Tristram-Nagle, S. & Nagle, J. F. Partial molecular volumes of lipids and cholesterol. *Chem. Phys. Lipids* **143**, 1–10 (2006).
29. Cvec, G. & Marsh, D. *Phospholipid bilayers*. pp. 347–361 (Wiley-Interscience, New York, 1990).
30. Stottrup, B. L., Veach, S. L. & Keller, S. L. Nonequilibrium behavior in supported lipid membranes containing cholesterol. *Biophys. J.* **86**, 2942–2950 (2004).
31. Edholm, O. & Nagle, J. F. Area of molecules in membranes consisting of mixtures. *Biophys. J.* **89**, 1827–1832 (2005).
32. Ali, S., Smaby, J. M., Brockman, H. L. & Brown, R. E. Cholesterol's interfacial interactions with galactosylceramides. *Biochemistry* **33**, 2900–2906 (1994).
33. Phillips, M. C. & Chapman, D. Monolayer characteristics of saturated 1,2-diacyl phosphatidylcholines (lecithins) and phosphatidylethanolamines at the air-water interface. *Biochim. Biophys. Acta* **163**, 301–313 (1968).
34. Demel, R. A., von Kessel, G., Zwaal, W. S. M., Roelofson, R. F. A. & van Deenen, L. L. M. Relation between various phospholipase actions on human red cell membranes and the interfacial phospholipid pressure in monolayers. *Biochim. Biophys. Acta* **406**, 97–107 (1975).
35. Evans, E. & Waugh, R. Mechano-chemistry of closed, vesicular membrane systems. *J. Colloid Interface Sci.* **60**, 286–298 (1997).
36. Blume, A. A comparative study of the phase transitions of phospholipid bilayers and monolayers. *Biochim. Biophys. Acta* **557**, 32–44 (1979).
37. Li, X. M., Momsen, M. M., Smaby, J. M., Brockman, H. L. & Brown, R. E. Cholesterol decreased the interfacial elasticity and detergent solubility of sphingomyelins. *Biochemistry* **40**, 5954–5963 (2001).
38. Almeida, R. F. M., Fedorov, A. & Prieto, M. Sphingomyelin/phosphatidylcholine/cholesterol phase diagram: Boundaries and composition of lipid raft. *Biophys. J.* **85**, 2406–2416 (2003).
39. Estep, T. N., Mountcastle, D. B., Barenholz, Y., Biltonen, R. L. & Tompson, T. E. Thermal behavior of synthetic sphingomyelin-cholesterol dispersions. *Biochemistry* **18**, 2112–2117 (1979).
40. Kim, M. Y., Linardic, C. M. Obeid, L. M. & Hannun, Y. Identification of sphingomyelin turnover as an effector mechanism for the action of tumor necrosis factor α and γ-interferon. *J. Biol. Chem*. **266**, 484–489 (1991).
41. Bielawska, A., Crane, H. M., Liotta, D., Obeid L. M. & Hannun, Y. A. Selectivity of ceramide mediated biology. *J. Biol. Chem*. **268**, 26226–26232 (1993).
42. Obeid, L. M., Linardic, C. M., Karolac, L. A. & Hannun, Y. A. Programmed cell death induced by ceramide. *Science* **259**, 1769–1771 (1993).
43. Rosenfeld, L. & Spector, A. Changes in lipid distribution in the human lens with the development of cataract. *Exp. Eye Res.* **33**, 641–650 (1981).
44. Cenedella, R. J. Cholesterol and cataract. *Surv. Ophthalmol*. **40**, 320–337 (1996).